Numerical simulations of Typhoon Chanthu (2021) by two nonhydrostatic atmosphere models and an atmosphere-wave ocean coupled model

Akiyoshi Wada, Wataru Yanase, and Satoki Tsujino

Meteorological Research Institute, Tsukuba, Ibaraki, 305-0052, JAPAN

[1]awada@mri-jma.go.jp

1. Introduction

A tropical depression developed to a tropical storm (named Chanthu) around (14.6°N, 138.0°E) at 12 UTC on 6 September 2021. Chanthu moved northwestward and then westward in its intensification phase. Chanthu reached the minimum central pressure of 905 hPa at 18 UTC on 10 September over the sea north of Luzon Island. Then, Chanthu changed the moving direction to the north and passed east of Taiwan while the tropical cyclone (TC) was weakening. The TC entered the East China Sea on 13 September and stagnated from 15 to 16 September. After the stagnation, the TC moved northeastward and made landfall in Japan around 18 UTC on 17 September.

There are two issues on the track forecast of Chanthu and the other two in the intensity forecast. First, the Japan Meteorological Agency (JMA) forecasted that Chanthu moved more northward than the observed track in the intensification phase. Second, the forecast error of the TC track increased on around 15 September in the East China Sea. Third, the JMA forecast tended to overly develop the TC during the mature and decaying phases. Last, the TC redeveloped in the East China Sea contrary to the forecast. This report addresses the second and third subjects. Numerical simulations were conducted for Chanthu by using an operational nonhydrostatic atmosphere model (asuca: Asuca is a System based on a Unified Concept for Atmosphere), a nonhydrostatic atmosphere model (NHM, Wada et al., 2018) and the coupled atmosphere-wave-ocean model (CPL, Wada et al., 2018).

2. Experimental design

Table 1 shows a list of numerical simulations. Each initial time was 0000 UTC on 9 September 2021. The computational domain was 1500 x 2700 km with a grid spacing of 1.5 km (Fig. 1a). The number of the vertical layer was 55 for NHM and CPL and 96 for asuca. The top height was approximately 27 km for the NHM and CPL and approximately 37 km for the asuca. The integration time of all simulations was 144 hours.

Table1 List of numerical simulations

Name	*Model*	*IRE*	*Cumulus Parameterization*
NHM	NHM	0.2	None
CPL	CPL	0.2	None
asuca(1.0)	asuca	1.0	KF: Kain and Fritsch (1990)
asuca(0.15)	asuca	0.15	KF: Kain and Fritsch (1990)
asuca(0.05)	asuca	0.05	KF: Kain and Fritsch (1990)

The time step was 3 seconds in the NHM, the asuca, and the atmospheric part of CPL, 18 seconds for the ocean model incorporated into the CPL, and 6 minutes for the ocean surface wave model incorporated into the CPL. The cumulus parameterization of Kain and Fritsch (1990) (KF in Table 1) was used only for the asuca. The setting of KF was the same as that in the local forecast model operationally used in JMA. The atmospheric boundary-layer scheme used in the NHM and CPL was the same as that in Wada et al. (2018), while Mellor-Yamada-Nakanishi-Niino level 2.5 closure scheme (e.g., Nakanishi and Niino, 2009) was used in the numerical simulations conducted by the asuca. The inhibition rate of evaporation (IRE) of rain, snow, and graupel included in the cloud physics for the NHM and CPL was 0.2, while three sensitivity experiments were conducted by the asuca on the IRE by using the following three values (1.0, 0.15, 0.05).

The JMA global objective analysis with the horizontal resolution of 20 km and the JMA North Pacific Ocean analysis with the horizontal resolution of 0.5° were used for creating atmospheric and oceanic initial conditions and atmospheric lateral boundary conditions every 6 hours. As for the initial condition of sea surface temperature (SST), the Optimally Interpolated SST (OISST) daily product with the horizontal resolution of 0.25°, obtained from the Remote Sensing Systems (http://www.remss.com) was used.

The Regional Specialized Meteorological Center (RSMC) Tokyo best track data (https://www.jma.go.jp/jma/jma-eng/jma-center/rsmc-hp-pub-eg/besttrack.html) was used to validate the results of numerical simulations.

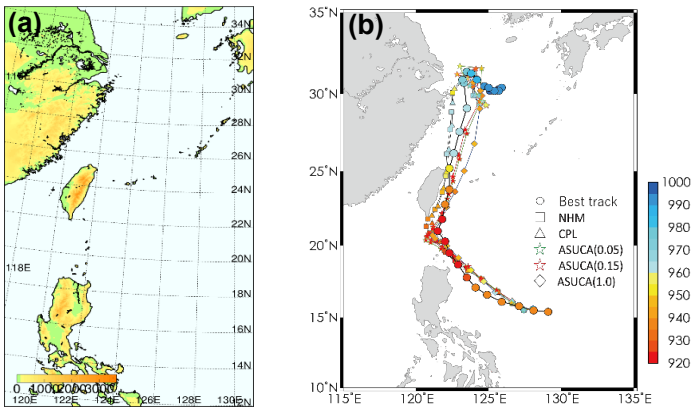

Figure 1 (a) Computational domain. (b) Track simulation results with the RSMC best track. Colors in the marks indicate the value of central pressure (hPa).

3. Results

3.1 Tracks

Figure 1b shows the results of simulated tracks and central pressures in all simulations together with the RSMC Tokyo best track data. All simulated tracks clearly show a northward deflection in the intensification phase compared to the best track when the TC actually moved westward. In the weakening phase of Chanthu, the variation in the simulated tracks among the simulations by the asuca with different IRE was greater than that in the intensification phase. The increase in IRE (from 0.05 to 1) in the simulations by the asuca led to the eastward shift of the simulated track. Compared to the impact of IRE on the tracks simulated by the asuca, there was less impact of ocean coupling on the tracks simulated by the NHM and CPL.

It should be noted that the value of 1.0 on IRE is scientifically valid. In other words, the discrepancy between the simulations and the best track suggests that the physical processes in the atmosphere models are not well-tuned.

3.2 Intensity changes

Figure 2 shows the time series of simulated central pressure with the best-track central pressure from 00 UTC on 9 September to 00 UTC on 15 September. The best-track central pressure at 00 UTC on 9 September was actually 935 hPa, which was much lower than the central pressure at the initial time obtained from objectively analysis with the horizontal resolution (20 km) much coarser than 1.5 km. The central pressure in the experiments asuca (0.05) and asuca (0.15) decreased more rapidly than that in the experiment asuca (1.0) at the early integration time. The rapid lowering was also simulated in the NHM and CPL experiments. The simulated central pressure simulated by the asuca decreased more rapidly for a lower IRE. However, the simulations by the NHM and CPL showed a relatively high value of the minimum central pressures although IRE was close to asuca (0.15). The impact of ocean coupling on simulated central pressures became distinct around 10 September.

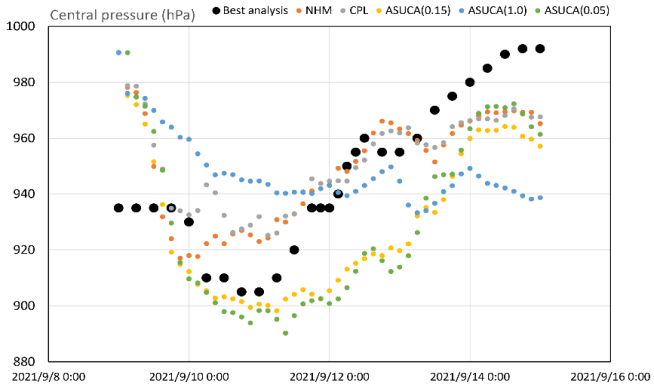

Figure 2 Time series of simulated central pressures with the best-track central pressure (hPa).

3.3 Wind structure in the inner core

Figure 3 shows the horizontal distributions of simulated winds at the height of 20 m. The wind distributions simulated by the NHM and CPL show the asymmetric distribution. The wind distribution simulated in the experiment asuca (1.0) also shows the asymmetric feature, while the axisymmetric feature was found in the wind distribution in the experiments asuca (0.05) and asuca (0.15). The difference in the surface wind distribution corresponded to the simulated intensity (Fig. 2) in that the simulated central pressure was relatively high when the surface wind distribution showed the asymmetric feature.

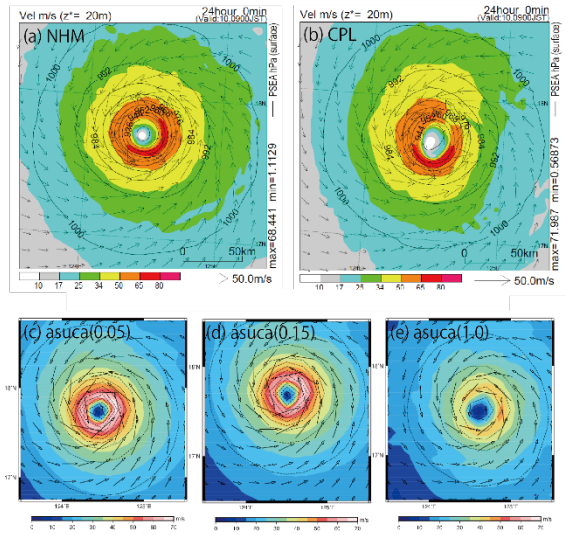

Figure 3 Horizontal distributions of winds at the height of 20 m at 00 UTC on 10 September 2021 simulated by the (a) NHM, (b) CPL and (c-e) asuca (see Table 1 for the difference in the inhibition rates of evaporation of rain, snow, and graupel).

4. Concluding remarks

The sensitivity to simulated TC to IRE may vary between the NHM and the asuca. In that sense, sensitivity to ocean coupling may also differ between the two models. The results of simulations by the asuca with different IRE suggest that the amount of evaporation cooling due to precipitation does affect the structure and track of simulated Chanthu. How this sensitivity will be changed by the asuca coupled with an ocean model will be a subject in the future.

If a TC in the mature phase is used as a case study, the initial condition should be realistically reproduced to avoid unrealistic decreases in central pressures.

References

Kain, J. S., and J. M. Fritsch (1990). A one-dimensional entraining/detraining plume model and its application in convective parameterization. Journal of the Atmospheric Sciences, 47, 2784-2802.

Nakanishi, M., and H. Niino (2009). Development of an improved turbulence closure model for the atmospheric boundary layer. Journal of the Meteorological Society of Japan, 87, 895-912.

Wada, A., S. Kanada, and H. Yamada (2018). Effect of air–sea environmental conditions and interfacial processes on extremely intense typhoon Haiyan (2013). Journal of Geophysical Research: Atmospheres, 123, 10379-10405.